

Abstract

The paper describes an artificial neural network method (ANNM) to predict the stresses executed on segmental tunnel lining. An ANN using multi-layer perceptron (MLP) is developed. At first, database resulted from numerical analyses was prepared. This includes; depth of cover (H), horizontal to vertical stress ratio (K), thickness of segment (t), Young modulus of segment (E) and key segment position in each ring (θ) on the tunnel perimeter as input variables. Different types of stresses and extreme values of displacement have been considered as output parameters. Sensitivity analysis showed that the cover of the tunnel and key position are the most and less effective input variables on output parameters, respectively. Results for coefficient of determination (R^2), variance accounted for (VAF), coefficient of efficiency (CE) and root mean squared error (RMSE) illustrates a high accuracy of the presented ANN model to predict the stress types and displacements of segmental tunnel lining.

Keywords

artificial neural network, tunnel, segment, lining, yield criterion

1 Introduction

Support lining of tunnels excavated by shield type of TBMs (Tunnel Boring Machine) is installed immediately after excavation of surrounding media. The support system of tunnel lining is composed of pre-casted reinforced concrete segments. Successive assembling of these concrete segments inside the TBM's shield, forms tunnel support rings. Design and construction of concrete segments are one of the most important steps in tunnel construction operation [1–4]. To simplify installing and assembling of ring erection operation, one segment is designed usually in trapezoidal shape which is smaller than the others and called key segment. Key segment will be installed at the end. Fig. 1 shows one assembled ring of concrete segments in segment manufacturing factory.



Fig. 1 An assembled concrete segmental ring, Segment factory, Tehran Metro-Line 4 [5]

Generally, design methods of tunnel lining can be classified in 3 different approaches: Analytical, Experimental and Numerical methods.

Analytical methods have been developed from the start of the tunnel support design history up to now [6–16]. Some of these analytical methods are restricted either to only elastic behaviour of tunnel lining and soil material or only to shallow tunnel conditions. Some others, taking into account few simple

¹School of Mining Engineering, College of Engineering, University of Tehran, Tehran, Iran

²School of Civil Engineering, College of Engineering, University of Tehran, Tehran, Iran

*Corresponding author, email: arminrastbood88@gmail.com

assumptions with reduced stiffness of segmental ring without consideration of longitudinal joints in reality. And some others do not consider smaller key segment size with respect to other segments in tunnel support ring and consider all of them with the same size.

Nowadays some attempts in design and analysis of segmental tunnel lining are carried out based on the laboratorial studies [17–23]. Other methods are often verified by experimental methods. The experimental methods are much more useful than analytical and numerical methods, but these methods are mostly time consuming and expensive.

Numerical methods have been developed widely in recent decades [24–29]. Numerical methods are often time consuming and need more detailed input data that could be unknown during analysis. Also these methods often need to advanced computer systems for analyzing. The results of numerical methods must be verified by either experimental, analytical methods or by in-situ monitoring results.

In recent years, to overcome with all above mentioned difficulties, new methods such as Fuzzy systems and Artificial Neural Network (ANN) models have been used as a prediction tool for analysis of complicated problems. ANN approach has been used widely in geotechnical and geomechanical engineering problems [30–42]. Due to above mentioned defects of numerical, experimental and analytical methods in design of segmental tunnel lining, application of ANN methods seems to be a new alternative solution as prediction tools.

Prediction of yield stresses and extreme values of tunnel lining ring displacement using ANN was not studied in detail as of yet. In this study, ANN method has been used to predict yield stresses and displacement of segmental tunnel lining ring based on the results obtained from numerical method. Sensitivity analysis of input variables performed to determine their effects on output results. Finally the performance of the model was evaluated by means of root mean squared error (RMSE) in percent (%), coefficient of determination (R^2), proportion of variance explained (PVE) or variance accounted for (VAF) in percent (%), and coefficient of efficiency (CE) indices.

2 Yield criteria

There are two most commonly used criteria in strength of materials: Von Mises and Tresca criteria. According to Von Mises yield criterion, material starts to yield once the second deviatoric stress invariant approaches to a critical value. In this criterion, Von Mises stress denoted by σ_v and when reaches to yield strength of material known as σ_y , it begins to yield. Von Mises stress can be calculated from Eq. (1) [43]:

$$\sigma_v^2 = 0.5 \times \left[(\sigma_{11} - \sigma_{22})^2 + (\sigma_{22} - \sigma_{33})^2 + (\sigma_{33} - \sigma_{11})^2 + 6(\sigma_{23}^2 + \sigma_{31}^2 + \sigma_{12}^2) \right] \quad (1)$$

Where:

σ_v : Von Mises stress;

σ_{ij} : Components of stress tensor.

Also, according to Tresca yield criterion, material starts to yield once maximum absolute value of shear stress in a material reaches to a critical value. It must be noticed that stress values of two yield criteria are calculated based on principal stress components. Comparison between both yield criteria is shown in Fig. 2.

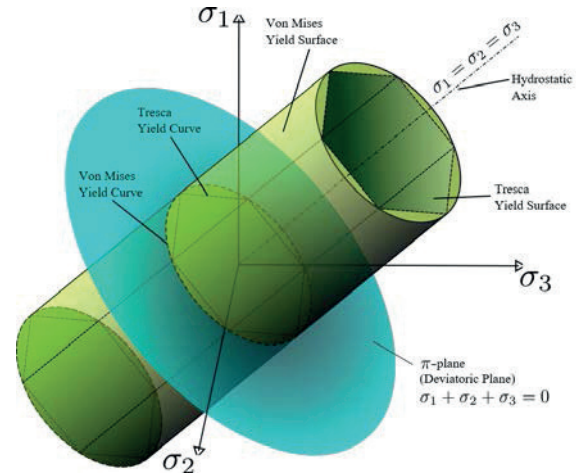


Fig. 2 Von Mises and Tresca yield surfaces [44]

3 Artificial neural network and multilayer perceptron

Artificial neural networks are composed of many data processing units called neurons. The aim of model is to simulate the act of human brain nature based on trial and error method using neurons [34, 45]. There are a large number of interconnections among the neurons in an ANN model. Generally speaking, a neural network model mostly composed of three layers in series, named: input layer, hidden layer(s) and output layer, respectively. Schematic view of a usual ANN is shown in Fig. 3. Hidden layer(s) is important layer of each neural network because the major calculation process is performed in this layer. Neurons on each layer are connected to the neurons of neighbouring layers with a coefficient named weight (w). Transform functions are used to transform the weighted sum of all input signals towards a neuron and calculate the output response of neuron. TANSIG and LOGSIG are two efficient non-linear sigmoid transform functions used in neural networks [37]. The output of an input layer is used as input for the hidden layer(s) and the same rule is applicable between hidden layer(s) and output layer, respectively. Optimum number of hidden layers and neurons are calculated based on trial and error rule and goal error value [34].

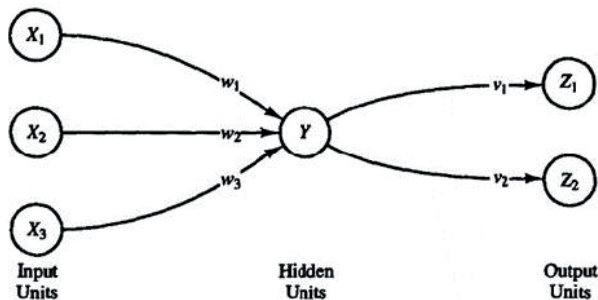


Fig. 3 Schematic view of a usual ANN [45]

At first, artificial neural network is trained by input data. Then tested and verified by other different input data. In training process, inputs are entered and outputs values are determined. Then error between predicted and real values is calculated. Based on these error values, the weights are adjusted by starting from the output layer towards the input layer. This process is known as Back Propagation (BP) algorithm. Back propagation algorithms are powerful tools for prediction models [45].

Perceptron neural net model proposed by Rosenblatt [46]. Then multiple layer perceptron neural network model was improved and proposed by Rumelhart [47]. In this model, the input layer normalizes input data values. This kind of data preparation and normalization, improves the network performances due to more homogeneous distribution of normalized data as shown in Fig. 4. This kind of normalization has been used by many researches [42, 46–49].

Except the input neurons, each neuron has a non-linear activation function. Multi-layer perceptron (MLP) is a modification of the standard linear perceptron, which can separate data that are not linearly separable [50].

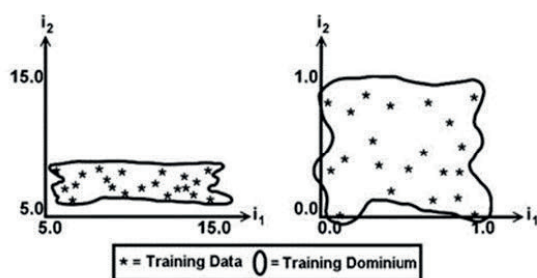


Fig. 4 Effect of data normalization on the homogeneity distribution [49]

4 Numerical modelling

To use an artificial neural network as prediction tool, at first should prepare comprehensive input data. Using this database, neural net will be trained, tested and validated. To do this, in this study the results obtained from finite element program (ABAQUS, [51]) were used as database. In designed numerical models, the support system of segmental tunnel lining is supposed to be one ring with 5 + 1 segments. The engineering and

geometrical properties of concrete segments are summarized in Table 1. Five concrete segments (named A2–A6) are almost similar to each other from geometrical point of view except key segment. To reduce the total time of numerical operation, soil elements are neglected in numerical model. Beam-spring method was used to model the tunnel lining structure [1, 2]. In this method the effects of soil body on tunnel lining and interaction between contact surfaces were simulated by means of tangential and radial springs. Tangential springs were neglected due to their negligible effects in comparison with radial springs. Stiffness of soil radial springs is calculated using Eq. (2), [52]:

$$K = \frac{A.E}{R.(1+\nu)} \quad (2)$$

Where:

K = stiffness of radial spring;

E = Young modulus of soil;

ν = poisson's ratio of soil;

R = tunnel radius; and

A = effective area of tunnel lining that is subjected to implied force from the soil, and calculated by Eq. (3):

$$A = R\theta.b \quad (3)$$

Where:

θ = radial angle between two successive radial springs, and

b = effective area of each spring in tunnel longitudinal direction.

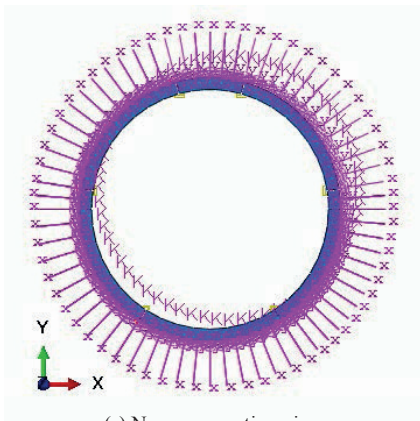
Figs. 5a–b show the non-perspective and perspective view of tunnel lining under soil imposed radial springs.

Table 1 Engineering and geometrical properties of concrete segments

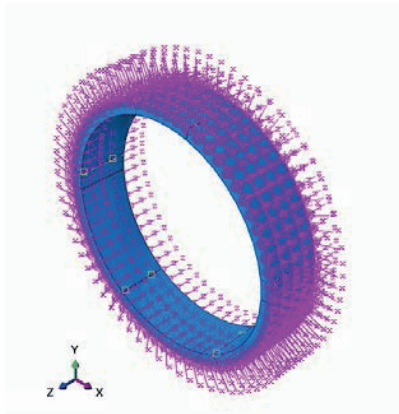
Segment No.	Engineering properties			Geometrical properties	
	E^*	ν^{**}	ρ^{***}	t^{****}	Central angle(°)
A1(key segment)	25	0.15	2350	30	30
A2-A6					66

*Young modulus (GPa), **poisson ratio, *** density (kg/m³), **** thickness(cm)

3D solid elements type was used to model the concrete segments. After assembling concrete segments to each other, plane strain condition was applied to the model. In this attempt, it is assumed that origin of angle in model plane is located at tunnel crown (Fig. 6a). Joints between two neighbouring segments named longitudinal joints .Fig. 6b shows longitudinal joints of assembled segments in a ring and the position of key segment at $\theta = 90^\circ$. The assembled ring presents the tunnel lining support system. Hard contact was supposed for six concrete to concrete contact surfaces between concrete segments with frictional penalty coefficient of 0.4.

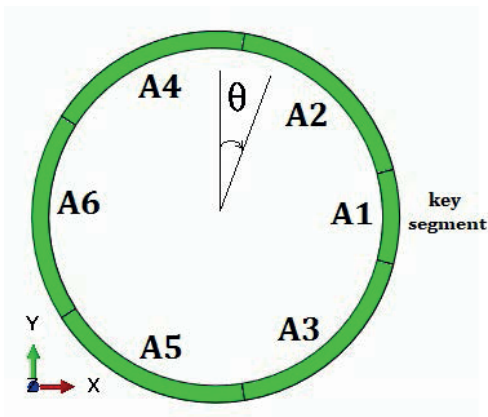


(a) Non-perspective view

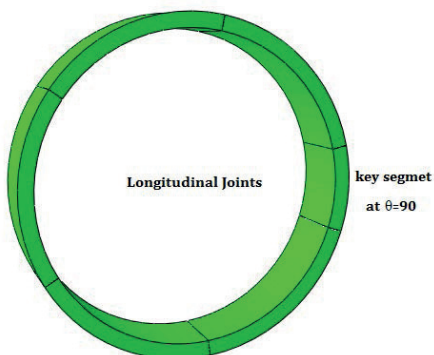


(b) perspective view

Fig. 5 Tunnel lining under soil imposed radial springs in radial direction

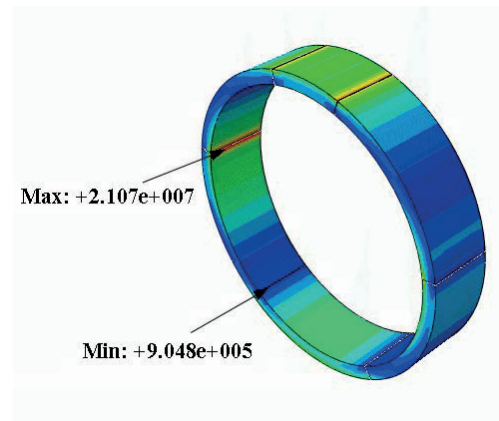


(a) Origin of θ angle

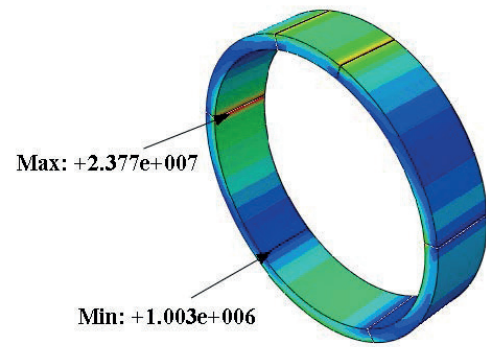


(b) Longitudinal joints and key position

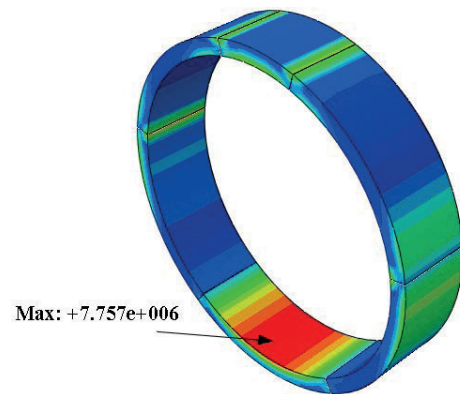
Fig. 6 Assembled ring of concrete segments



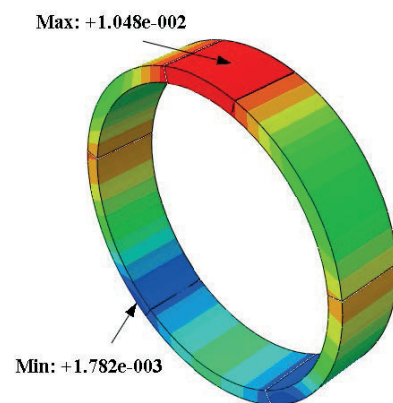
(a) Extreme Values of Von Mises Stresses (N/m²)



(b) Extreme Values of Tresca Stresses (N/m²)



(c) Maximum Value of maximum principal Stress (N/m²)



(d) Extreme values of ring displacement (m)

Fig. 7 Von Mises and Tresca stresses with principal stresses and extreme values of ring displacements

5 Data collection and preparation for artificial neural network

The numerical model at first was solved for $t=30\text{cm}$, overburden $H = 5\text{m}$, $K = 0.5$ (horizontal to vertical stress ratio), $E = 25\text{ Gpa}$ and $\theta = 0^\circ$. Then t , H , K and E values were kept constant and θ value changed 30° , 60° , 90° , 120° , 150° and 180° respectively. To prepare database, for each value of input variables, values of other input variables were changed according to values mentioned in Table 2. Table 2 shows the times of changes of each input variable and their magnitudes. Key positions at 210° , 240° , 270° , 300° and 330° at tunnel periphery were neglected due to the axisymmetric shape of tunnel lining ring. Finally 252 numerical models were analyzed. Some randomly selected input data variables and resulted outputs are summarized in Table 3. Figs. 7a–d show the values resulted for Von Mises and Tresca stresses together with principal stresses and extreme values of ring displacements for $t = 30\text{cm}$, $H = 15\text{m}$, $K = 0.5$, $E = 20\text{ Gpa}$ and $\theta = 0^\circ$.

Table 2 Different values for input variables

Different values of 5 Input Variables				
t (cm)	H(m)	K	E(GPa)	Key Position(°)
30	5	0.5	25	0
				30
				60
				90
				120
40	15	1.0	35	150
				180
				210
				240
				270
	25	1.5		300
				330
				360
				390
				420

Number of total numerical models: $2*3*3*2*7=252$.

6 Application of ANN

6.1 Data Normalization

To increase the processing and convergence rate during training process and to minimize the prediction error, raw data must be normalized [53]. Before modelling commences, all data should be checked and any false data must be deleted. Then data should be normalized to bring all of the variables into proportion with one another. To normalize data, traditionally this means to fit the data within unity, so all data values will be in the range of 0 to 1.

Equation 4 is what should be used to implement a unity-based normalization [54]:

$$u_{Norm} = \frac{u - u_{min}}{u_{max} - u_{min}} \quad (4)$$

Where:

u : any raw data

u_{Norm} : normalized data

u_{min} : minimum value of data

u_{max} : maximum value of data

6.2 Optimum architecture of MLP Model

Obtained data from numerical modelling were used to prepare the multi-layer perceptron model for prediction aim. In this study, data were divided into 3 parts: training data (70% of total data), testing data (20% of total data) and validation data (10% of total data). The optimum structure (number of hidden layers) and optimum number of neurons in hidden layers of neural network model could be determined based on trial and error rule.

At first, the optimum numbers of neurons were calculated based on RMSE values. Then, obtained optimum number of neurons were embedded on hidden layers of the model.

RMSE value was calculated according to Eq. (5):

$$RMSE = \sqrt{\frac{1}{N} \cdot \sum_{i=1}^N (\hat{u}_k - u_k)^2} \quad (5)$$

Where:

RMSE = Root mean square error value;

\hat{u}_k and u_k = the k th predicted and observed values of target, respectively; and

N = the number of observations for which the error has been computed

The obtained results are illustrated on Fig. 8. It can be seen that the minimum value of RMSE was obtained by 11 number of neurons. Also there are some relation to estimate number of neurons in hidden layers. These relations are presented in Table 4.

So, the obtained number of neurons for hidden layers by RMSE value is in accordance with Hecht-Nielsen (1987) and Kanellopoulas and Wilkinson (1997).

Table 3 Randomly selected raw data obtained from finite element method

No	Input variables					Output parameters							
	t ¹	H ²	K	E ³	θ ⁴	MisesMax ⁵	MisesMin ⁶	TrescaMax ⁷	TrescaMin ⁸	MaxPrinMax ⁹	MinPrinMin ¹⁰	UMax ¹¹	UMin ¹²
1	30	5	0.5	20	0	3.003E+06	3.606E+05	3.269E+06	4.065E+05	8.101E+05	-2.896E+06	5.132E-03	2.151E-03
2	30	5	0.5	20	30	2.768E+06	3.356E+05	3.019E+06	3.801E+05	8.818E+05	-2.686E+06	5.211E-03	2.178E-03
3	30	5	0.5	20	60	3.099E+06	3.148E+05	3.381E+06	3.426E+05	9.302E+05	-2.957E+06	5.242E-03	2.189E-03
4	30	5	0.5	20	90	2.685E+06	3.432E+05	2.917E+06	3.586E+05	8.315E+05	-2.616E+06	5.117E-03	2.162E-03
5	30	5	0.5	20	120	2.973E+06	2.976E+05	3.248E+06	3.256E+05	8.148E+05	-2.833E+06	5.087E-03	2.144E-03
6	30	5	0.5	20	150	2.710E+06	2.738E+05	2.967E+06	3.147E+05	8.246E+05	-2.618E+06	5.175E-03	2.115E-03
7	30	5	0.5	20	180	3.181E+06	3.433E+05	3.469E+06	3.861E+05	9.749E+05	-3.045E+06	5.285E-03	2.132E-03
8	30	5	0.5	35	0	3.389E+06	3.500E+05	3.708E+06	3.944E+05	9.477E+05	-3.208E+06	4.844E-03	2.459E-03
9	30	5	0.5	35	30	3.111E+06	3.369E+05	3.414E+06	3.746E+05	1.005E+06	-2.952E+06	4.909E-03	2.488E-03
10	30	5	0.5	35	60	3.495E+06	2.829E+05	3.832E+06	3.057E+05	1.066E+06	-3.274E+06	4.932E-03	2.498E-03
11	30	5	0.5	35	90	2.967E+06	3.486E+05	3.250E+06	3.768E+05	9.618E+05	-2.840E+06	4.827E-03	2.468E-03
12	30	5	0.5	35	120	3.322E+06	2.633E+05	3.646E+06	2.864E+05	9.523E+05	-3.111E+06	4.799E-03	2.454E-03
13	30	5	0.5	35	150	3.081E+06	2.732E+05	3.390E+06	3.096E+05	9.500E+05	-2.912E+06	4.866E-03	2.423E-03
14	30	5	0.5	35	180	3.599E+06	3.182E+05	3.945E+06	3.557E+05	1.124E+06	-3.382E+06	4.964E-03	2.437E-03
15	30	5	1	20	0	8.973E+06	4.509E+05	1.015E+07	5.100E+05	2.848E+06	-7.312E+06	6.902E-03	4.194E-04
16	30	5	1	20	30	7.944E+06	5.206E+05	8.911E+06	5.938E+05	2.746E+06	-6.734E+06	6.864E-03	7.393E-04
17	30	5	1	20	60	1.134E+07	4.351E+05	1.293E+07	4.781E+05	3.945E+06	-8.995E+06	6.759E-03	5.849E-04
18	30	5	1	20	90	8.703E+06	4.545E+05	9.776E+06	4.970E+05	2.894E+06	-7.289E+06	6.881E-03	5.465E-04
19	30	5	1	20	120	1.147E+07	5.259E+05	1.307E+07	5.905E+05	3.992E+06	-9.080E+06	6.969E-03	6.338E-04
20	30	5	1	20	150	8.778E+06	4.737E+05	9.860E+06	4.880E+05	2.767E+06	-7.324E+06	6.608E-03	5.002E-04
21	30	5	1	20	180	9.077E+06	4.402E+05	1.027E+07	5.077E+05	2.885E+06	-7.385E+06	6.720E-03	6.167E-04
22	30	5	1	35	0	9.247E+06	4.245E+05	1.043E+07	4.897E+05	2.853E+06	-7.582E+06	6.505E-03	7.223E-04
23	30	5	1	35	30	9.216E+06	5.048E+05	1.038E+07	5.628E+05	3.108E+06	-7.597E+06	6.393E-03	1.244E-03
24	30	5	1	35	60	1.132E+07	4.293E+05	1.290E+07	4.570E+05	3.932E+06	-8.981E+06	6.313E-03	9.942E-04
25	30	5	1	35	90	1.008E+07	4.743E+05	1.137E+07	5.208E+05	3.295E+06	-8.219E+06	6.394E-03	9.874E-04
26	30	5	1	35	120	1.144E+07	4.971E+05	1.305E+07	5.261E+05	3.982E+06	-9.065E+06	6.544E-03	1.071E-03
27	30	5	1	35	150	9.590E+06	4.726E+05	1.080E+07	5.169E+05	3.122E+06	-7.878E+06	6.123E-03	9.020E-04
28	30	5	1	35	180	9.061E+06	4.277E+05	1.025E+07	4.911E+05	2.880E+06	-7.373E+06	6.446E-03	9.922E-04
29	30	5	1.5	20	0	1.234E+07	5.647E+05	1.397E+07	6.210E+05	5.764E+06	-1.001E+07	1.704E-02	3.298E-03
30	30	5	1.5	20	30	1.240E+07	6.540E+05	1.410E+07	7.162E+05	6.406E+06	-9.928E+06	2.114E-02	2.149E-03
31	30	5	1.5	20	60	1.479E+07	5.160E+05	1.689E+07	5.683E+05	5.249E+06	-1.171E+07	1.825E-02	3.144E-03
32	30	5	1.5	20	90	1.301E+07	6.011E+05	1.467E+07	6.731E+05	7.632E+06	-1.064E+07	1.915E-02	2.543E-03
33	30	5	1.5	20	120	1.494E+07	7.053E+05	1.706E+07	7.854E+05	5.285E+06	-1.181E+07	1.929E-02	2.461E-03
34	30	5	1.5	20	150	1.239E+07	6.031E+05	1.394E+07	6.376E+05	6.190E+06	-1.020E+07	1.568E-02	2.862E-03
35	30	5	1.5	20	180	1.256E+07	5.746E+05	1.417E+07	6.298E+05	5.527E+06	-1.029E+07	1.734E-02	2.947E-03
36	30	5	1.5	35	0	1.239E+07	5.671E+05	1.404E+07	6.249E+05	5.854E+06	-1.005E+07	1.712E-02	3.307E-03
37	30	5	1.5	35	30	1.247E+07	6.570E+05	1.417E+07	7.202E+05	6.614E+06	-9.975E+06	2.187E-02	1.996E-03
38	30	5	1.5	35	60	1.482E+07	5.173E+05	1.692E+07	5.694E+05	5.261E+06	-1.173E+07	1.853E-02	2.996E-03
39	30	5	1.5	35	90	1.306E+07	6.036E+05	1.472E+07	6.760E+05	7.735E+06	-1.068E+07	1.961E-02	2.526E-03
40	30	5	1.5	35	120	1.497E+07	6.976E+05	1.709E+07	7.512E+05	5.297E+06	-1.184E+07	2.000E-02	2.291E-03
41	30	5	1.5	35	150	1.243E+07	6.054E+05	1.398E+07	6.416E+05	6.347E+06	-1.023E+07	1.555E-02	2.847E-03
42	30	5	1.5	35	180	1.259E+07	5.764E+05	1.421E+07	6.331E+05	5.616E+06	-1.032E+07	1.753E-02	2.813E-03
43	30	15	0.5	20	0	2.107E+07	9.048E+05	2.377E+07	1.003E+06	7.757E+06	-1.720E+07	1.408E-02	1.782E-03
44	30	15	0.5	20	30	1.896E+07	9.841E+05	2.142E+07	1.098E+06	6.697E+06	-1.550E+07	1.389E-02	2.147E-03
45	30	15	0.5	20	60	2.001E+07	6.141E+05	2.253E+07	6.691E+05	7.341E+06	-1.645E+07	1.360E-02	1.623E-03
46	30	15	0.5	20	90	1.981E+07	8.458E+05	2.237E+07	9.639E+05	7.000E+06	-1.617E+07	1.538E-02	2.304E-03
47	30	15	0.5	20	120	1.900E+07	6.059E+05	2.142E+07	6.585E+05	7.262E+06	-1.565E+07	1.269E-02	2.211E-03
48	30	15	0.5	20	150	1.963E+07	8.339E+05	2.200E+07	9.062E+05	6.732E+06	-1.629E+07	1.617E-02	1.939E-03
49	30	15	0.5	20	180	2.115E+07	8.803E+05	2.385E+07	9.776E+05	7.935E+06	-1.725E+07	1.358E-02	2.112E-03
50	30	15	0.5	35	0	2.115E+07	9.818E+05	2.385E+07	1.089E+06	9.086E+06	-1.727E+07	1.333E-02	1.389E-03
51	30	15	0.5	35	30	2.177E+07	1.076E+06	2.465E+07	1.193E+06	7.468E+06	-1.757E+07	1.336E-02	2.070E-03
52	30	15	0.5	35	60	2.009E+07	6.163E+05	2.261E+07	6.718E+05	7.719E+06	-1.651E+07	1.349E-02	1.452E-03
53	30	15	0.5	35	90	1.981E+07	9.563E+05	2.237E+07	1.045E+06	8.186E+06	-1.616E+07	1.501E-02	1.994E-03
54	30	15	0.5	35	120	1.909E+07	6.081E+05	2.152E+07	6.607E+05	7.804E+06	-1.570E+07	1.306E-02	2.101E-03
55	30	15	0.5	35	150	1.964E+07	8.337E+05	2.200E+07	9.059E+05	7.122E+06	-1.631E+07	1.638E-02	1.772E-03
56	30	15	0.5	35	180	2.122E+07	9.591E+05	2.393E+07	1.077E+06	9.260E+06	-1.732E+07	1.243E-02	2.041E-03
57	30	15	1	20	0	7.361E+06	1.625E+06	7.910E+06	1.876E+06	1.155E+06	-7.454E+06	6.249E-03	1.231E-03
58	30	15	1	20	30	7.331E+06	1.792E+06	7.884E+06	2.020E+06	1.204E+06	-7.414E+06	6.195E-03	1.239E-03
59	30	15	1	20	60	7.499E+06	1.590E+06	8.204E+06	1.836E+06	1.198E+06	-7.695E+06	6.138E-03	1.250E-03
60	30	15	1	20	90	7.419E+06	1.608E+06	7.967E+06	1.840E+06	1.224E+06	-7.516E+06	6.204E-03	1.213E-03

(Units - 1: cm, 2: m, 3: GPa, 4: °, 5-10: N/m², 11-12:m)

Table 4 Determination of neurons for hidden layers of neural networks

Reference	Equation	This Study
Hush, 1989[55]	$3*N.I.N^1$	15
Hecht-Nielsen, 1987[56]	$\geq 2*N.I.N + 1$	≥ 11
Kanellopoulas and Wilkinson, 1997 [57]	$2*N.I.N$	10
Wang C, 1994[58]	$2*N.I.N/3$	≈ 3
Masters, 1994 [59]	$(N.I.N*N.O.N^2)^{0.5}$	≈ 2

1: N.I.N: Number of Input Neurons; 2: N.O.N: Number of Output Neurons

Thereafter, these neurons must be arranged in one or two hidden layer. Theoretically, only one hidden layer is enough for networks with Back Propagation (BP) algorithms [45, 56], but to solve some problems a neural network with two hidden layers is required [45, 59]. In some cases, application of neural networks with more than two hidden layers is useful [57]. Flood and Kartan [49] stated that MLP model with at least two hidden layers provides more flexibility for modelling complex problems. So, different arrangement of 11 neurons were considered in two hidden layers. Based on two transform functions (TANSIG and LOGSIG) resulted RMSE values are summarized in Table 5. It can be seen that model has the best performance in 5-7-4-1 neuron arrangement based on minimum RMSE value.

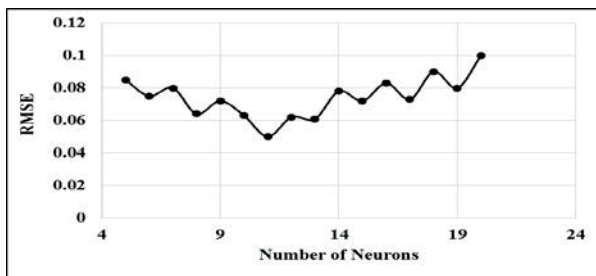


Fig. 8 Optimum number of neurons in hidden layer(s) based on minimum value for RMSE

Table 5 Optimum arrangement of neurons in two hidden layers

No.	Network Arrangement	RMSE Error	
		Transfer Function: TANSIG	Transfer Function: LOGSIG
1	5-[3-8]-1	0.123	0.119
2	5-[4-7]-1	0.082	0.098
3	5-[5-6]-1	0.075	0.088
4	5-[6-5]-1	0.053	0.060
5	5-[7-4]-1	0.041	0.055
6	5-[8-3]-1	0.074	0.085

Input layer
5 Neurons

Hidden layer I
7 Neurons

Hidden layer II
4 Neurons

Output layer
1 Neuron

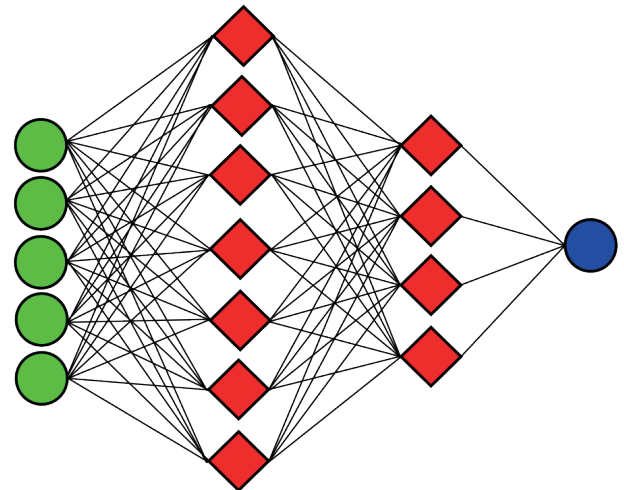


Fig. 9 Optimized structure of the artificial neural network

7 Sensitivity Analysis

Sensitivity analysis was performed to identify the influence of each input variable on output parameters. A useful method is the CAM (cosine amplitude method) [60, 61]. Data samples form a data vector, X , defined as:

$$X = \{x_1, x_2, x_3, \dots, x_n\}$$

Each of the components x_i in the data vector X , is a vector with length m , i.e.,

$$x_i = \{x_{i1}, x_{i2}, x_{i3}, \dots, x_{im}\}$$

Hence, each data can be assumed as a point in m -dimensional space, where each point needs m coordinates for a full description. Each element of a relation, r_{ij} , results from a pairwise comparison of two data pairs, i.e. x_i and x_j , where the strength of the relationship between data sample x_i and data sample x_j is defined according to Eq. (6):

$$r_{ij} = \frac{\left| \sum_{k=1}^m x_{ik} x_{jk} \right|}{\sqrt{\left(\sum_{k=1}^m x_{ik}^2 \right) \left(\sum_{k=1}^m x_{jk}^2 \right)}} \quad (6)$$

Where:

r_{ij} = strength values of relations between input variables and output parameters, and

$$i, j = 1, 2, \dots, n.$$

According to Eq. (6) this method is related to the dot product for the cosine function. When two vectors are collinear (most similar), dot product will be unity; when the two vectors are perpendicular to each other (most dissimilar), dot product will be zero [61].

Figs. 10–17 show the strength values of relations (r_{ij}) between input variables (t, H, K, E, θ) and output parameters.

As can be seen from these figures, effectiveness of all input variables have nearly same values. Nevertheless, for all output parameters, overburden of buried tunnel (H) is the most effective parameter than other four input variable, and θ value (position of key segment) has the least effect on output parameters.

8 Model performance

Performance of each ANN model must be calculated in predicting ability of output values. To do this, four performance indices including coefficient of determination (R^2), proportion of variance explained (PVE) or variance accounted for (VAF), coefficient of efficiency (CE) and root mean squared error (RMSE) were selected and calculated based on testing data sets. These data sets selected randomly from database and not included in the model training. VAF and CE values are calculated using Eq. (7) and Eq. (8):

$$VAF = 100 \times \left(1 - \frac{\text{var}(u_k - \hat{u}_k)}{\text{var}(u_k)} \right) \quad (7)$$

$$CE = 1 - \frac{\sum_{k=1}^N (\hat{u}_k - u_k)^2}{\sum_{k=1}^N (\hat{u}_k - \bar{\hat{u}}_k)^2} \quad (8)$$

Where:

var is the variance; \hat{u}_k and u_k are the k_{th} predicted and measured values respectively;

$\bar{\hat{u}}_k$ is the average of predicted values; and N is the number of data.

VAF index express the degree of difference between the variances of measured and predicted data sets. The values of VAF closer to 100 % indicate low variability and consequently better prediction capabilities. The lower the RMSE, the better the model performs [62, 63]. In ideal condition, the value of RMSE should be zero and value of CE should be unity. Obtained values for these indices are presented in Table 6. Also the graphs of correlation coefficient (R^2) for each type of input data (all data, training, test and validation) for output parameters are presented in Figs. 18–25. Relationship between output and target values for each type of input data and each output parameter are presented next to the related graphs. Obtained results show that minimum value of correlation coefficient relates to the minimum displacement of the ring (Fig. 25). However all obtained values show that generally high correlation is governed between all output and target values.

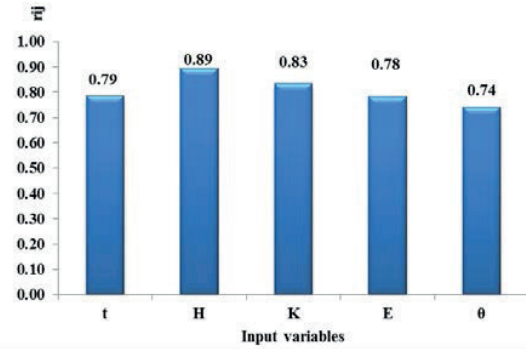


Fig. 10 Sensitivity analysis of Maximum Mises stress

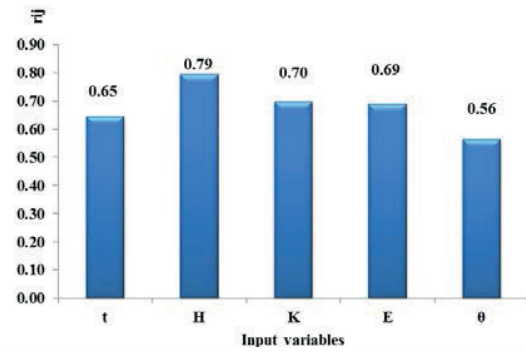


Fig. 11 Sensitivity analysis of minimum Mises stress

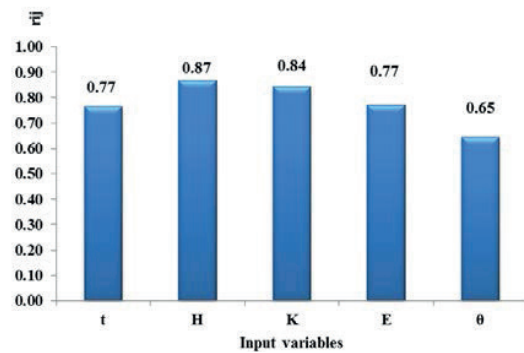


Fig. 12 Sensitivity analysis of maximum Tresca stress

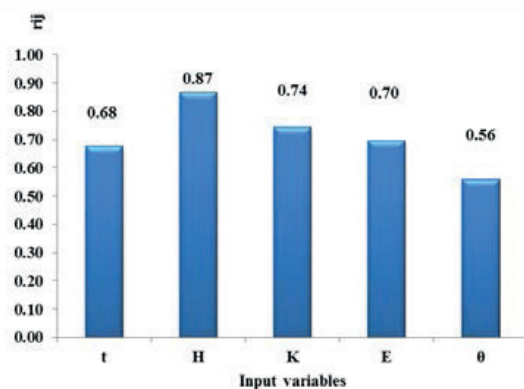


Fig. 13 Sensitivity analysis of minimum Tresca stress

Table 6 Performance indices of the neural network model

Performance Index	Output parameters							
	MisesMax	MisesMin	TrescaMax	TrescaMin	MaxPrinMax	MinPrinMin	UMax	UMin
RMSE (%)	3	6	4	4	5	3	5	5
R2 (%)	98	95	98	98	97	99	97	93
VAF (%)	98	95	98	98	97	99	97	93
CE	97	95	98	98	97	99	97	93

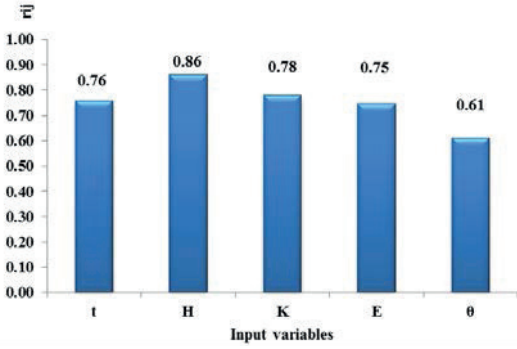


Fig. 14 Sensitivity analysis of maximum principal stress

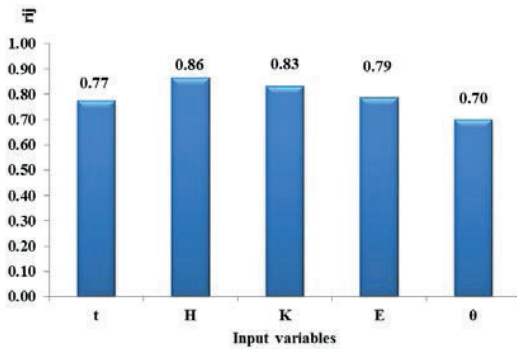


Fig. 15 Sensitivity analysis of minimum principal stress

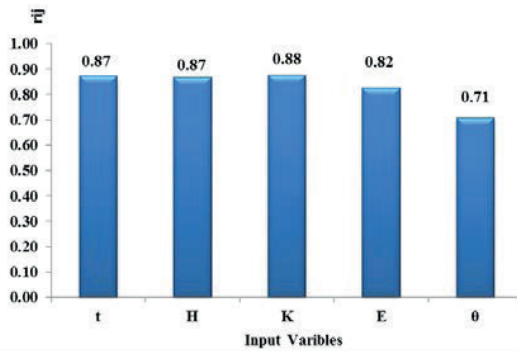


Fig. 16 Sensitivity analysis of maximum displacement

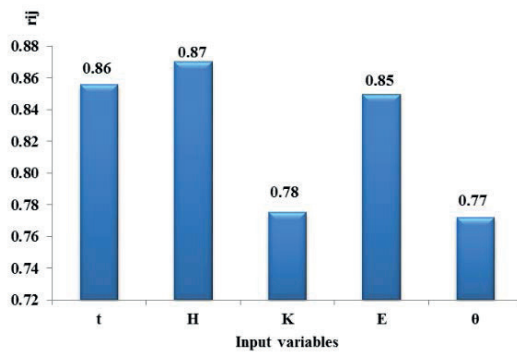


Fig. 17 Sensitivity analysis of minimum displacement

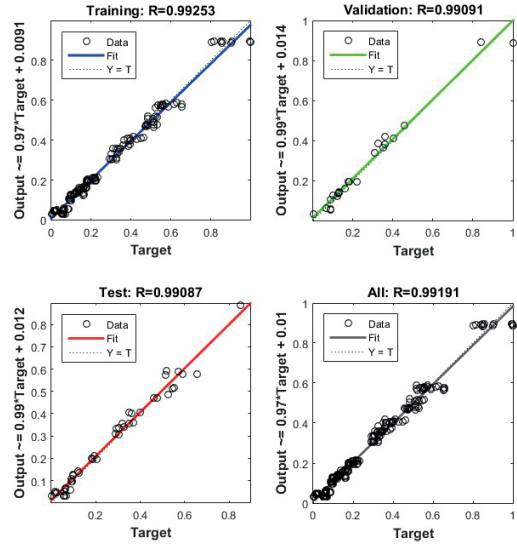


Fig. 18 Correlation coefficient for maximum Mises stress

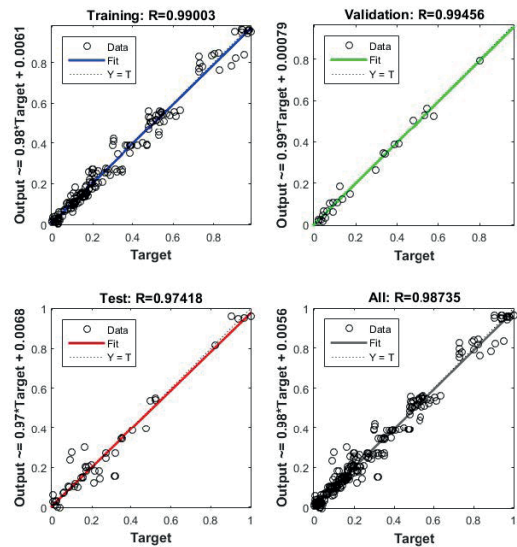


Fig. 19 Correlation coefficient for minimum Mises stress

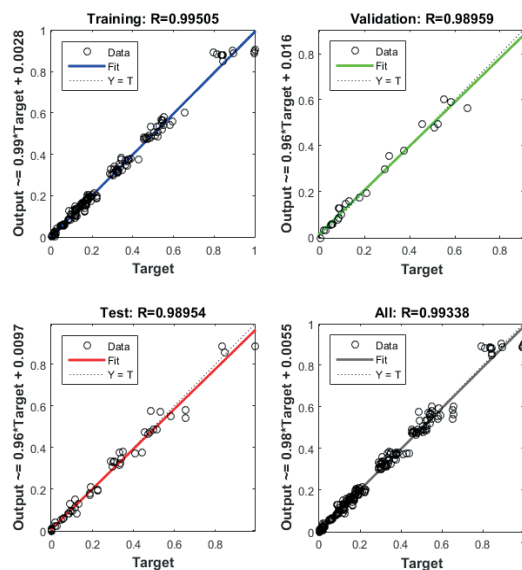


Fig. 20 Correlation coefficient for maximum Tresca stress

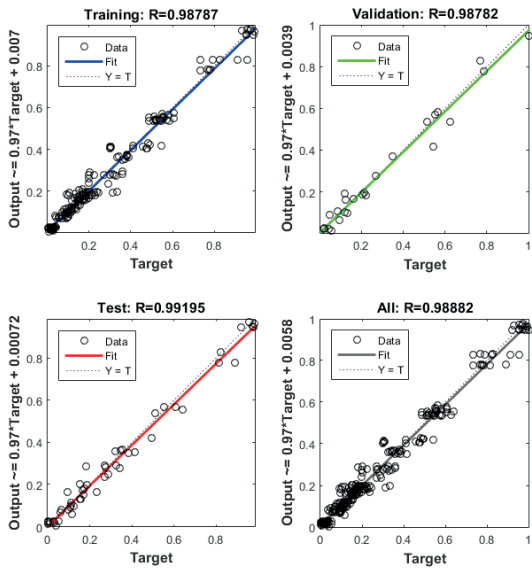


Fig. 21 Correlation coefficient for minimum Tresca stress

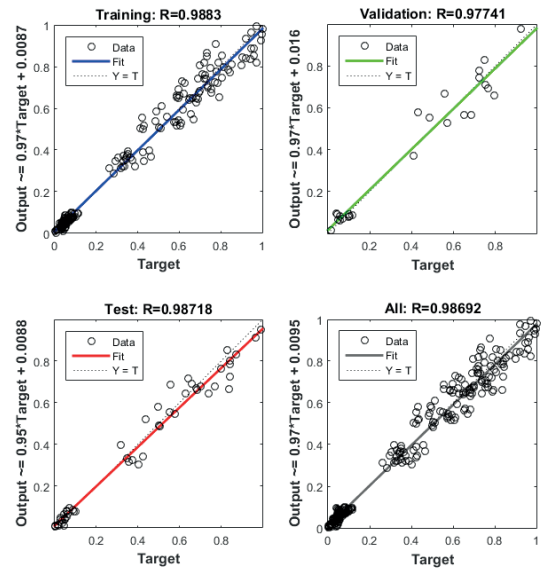


Fig. 24 Correlation coefficient for Maximum displacement

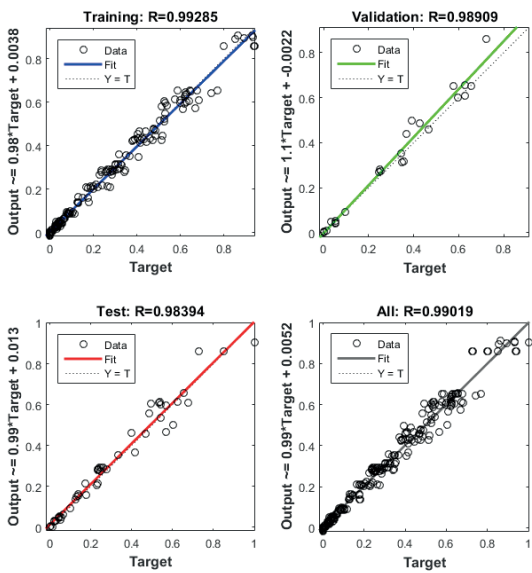


Fig. 22 Correlation coefficient for Maximum value of maximum Principal stress

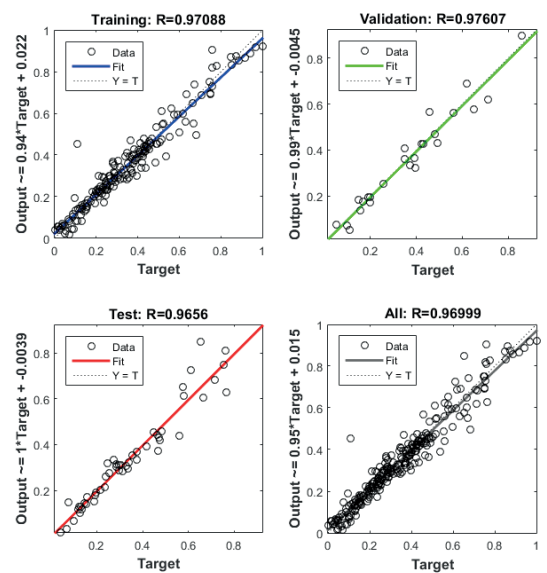


Fig. 25 Correlation coefficient for Minimum displacement

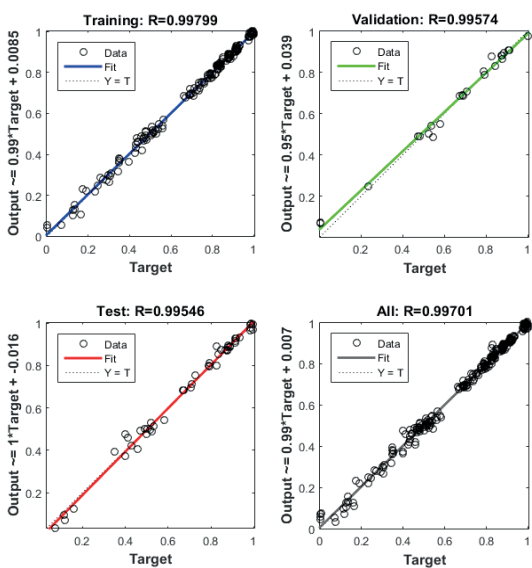


Fig. 23 Correlation coefficient for Minimum value of minimum Principal stress

9 Conclusions

To achieve knowledge about the safety of the support system of tunnel lining ring, von Mises and Tresca stresses together with principal stresses and extreme values of ring displacements were determined using finite element method. A segmental tunnel lining ring with 5+1 segments is modelled. To prepare enough data for ANN, parametric analysis was done. 252 numerical models were solved. After preparation of sufficient required input data, multi-layer perceptron neural net was selected as prediction model. Firstly, number of neurons and their arrangement in two hidden layers were optimized based on minimum obtained values for RMSE from input data variables. The minimum value of RMSE was 0.05 for 11 number of neurons. This obtained value for number of neurons in hidden layers was in conformity with the presented relations in literature. Consequently, in 5-7-4-1 structure arrangement of neural net model, resulted minimum value for RMSE was 0.041 and 0.055 for transfer functions of TANSIG and LOGSIG, respectively. Then the model tested and validated using different datasets. Sensitivity analyses were performed to determine the influence of each input variable on different types of output parameters. The obtained results were as below:

- Although sensitivity analysis showed that all the input variables have nearly same value of influence on the output parameters, but in all conditions, Height (H) and θ input variables are the most and less effective parameters on outputs parameters than three other input variables, respectively.
- Also the performance of presented model was evaluated using RMSE, R^2 , VAF and CE indices. Obtained results showed the excellent ability of the presented model in prediction of different type of stresses and extreme values of ring displacement and this prediction model can be used in high accuracy to obtain reliable results for preliminary study and design of segmental tunnel lining instead of current time consuming and expensive methods.

References

- [1] Japan Society of Civil Engineers. "Japanese Standard for Shield Tunnelling". JSCE, Tokyo, Japan. 1996.
- [2] Working Group No. 2, International Tunnelling Association. "Guidelines for the design of shield tunnel lining". *Tunnelling and Underground Space Technology*, 15(3), pp. 303–331. 2000. [https://doi.org/10.1016/S0886-7798\(00\)00058-4](https://doi.org/10.1016/S0886-7798(00)00058-4)
- [3] O'Carroll, J. B. "A Guide to Planning, Constructing, and Supervising Earth Pressure Balance TBM Tunneling". Parsons Brinckerhoff, New York. 2005.
- [4] Wittke, W., Erichsen, C., Gattermann, J. "Stability Analysis and Design for Mechanized Tunnelling". WBI, Felsbau GmbH, Aachen. 2006.
- [5] Majdi, A., Ajamzadeh, H., Kiani, M. "Numerical evaluation of the influence of bolted-and non-bolted joints on segmental tunnel lining behavior in line 4 Tehran subways.". In: ISRM International Symposium - 6th Asian Rock Mechanics Symposium, New Delhi, India, Oct. 23–27, 2010. <https://www.onepetro.org/conference-paper/ISRM-ARMS6-2010-106>
- [6] Morgan, H. "A contribution to the analysis of stress in a circular tunnel". *Geotechnique*, 11(1), pp. 37–46. 1961. <https://doi.org/10.1680/geot.1961.11.1.37>
- [7] Wood, A. M. "The circular tunnel in elastic ground". *Geotechnique*, 25(1), pp. 115–127. 1975. <https://doi.org/10.1680/geot.1975.25.1.115>
- [8] Ranken, R. E. "Analysis of ground-liner interaction for tunnels.". PhD dissertation, 1978. <https://www.ideals.illinois.edu/handle/2142/66846>
- [9] Einstein, H. H., Schwartz, C. W. "Simplified analysis for tunnel supports". *Journal of Geotechnical and Geoenvironmental Engineering*, 105 (GT4), pp. 499–518. 1979. <https://trid.trb.org/view.aspx?id=86688>
- [10] Duddeck, H., Erdmann, J. "Structural design models for tunnels in soft soil". *Underground Space*, 9, pp. 5–6. 1985. <https://www.osti.gov/scitech/biblio/7136781>
- [11] Koyoma, Y., Nishimura, T. "The design of lining segment of shield tunnel using a beam-spring model". *Railway Technical Research Institute, Quarterly Reports*, 39(1), pp. 23–27. 1998. <https://trid.trb.org/view.aspx?id=477386>
- [12] Penzien, J., Wu, C. L. "Stresses in linings of bored tunnels". *Earthquake Engineering & Structural Dynamics*, 27(3), pp. 283–300. 1998. [https://doi.org/10.1002/\(SICI\)1096-9845\(199803\)27:3%3C283::AID-EQE732%3E3.0.CO;2-T](https://doi.org/10.1002/(SICI)1096-9845(199803)27:3%3C283::AID-EQE732%3E3.0.CO;2-T)
- [13] Lee, K., Ge, X. "The equivalence of a jointed shield-driven tunnel lining to a continuous ring structure". *Canadian Geotechnical Journal*, 38(3), pp. 461–483. 2001. <https://doi.org/10.1139/t00-107>
- [14] You, X., Zhang, Z., Li, Y. "An analytical solution of shield tunnel based on force method.". In: *Underground Space - The 4th Dimension of Metropolises, Three Volume Set +CD-ROM*. Chapter 131. CRC Press. 2007. <https://doi.org/10.1201/NOE0415408073.ch131>
- [15] El Naggar, H., Hinchberger, S. D. "An analytical solution for jointed tunnel linings in elastic soil or rock". *Canadian Geotechnical Journal*, 45(11), pp. 1572–1593. 2008. <https://doi.org/10.1139/T08-075>
- [16] El Naggar, H., Hinchberger, S. D., Lo, K. "A closed-form solution for composite tunnel linings in a homogeneous infinite isotropic elastic medium". *Canadian Geotechnical Journal*, 45(2), pp. 266–287. 2008. <https://doi.org/10.1139/T07-055>
- [17] Mashimo, H., Ishimura, T. "Evaluation of the load on shield tunnel lining in gravel". *Tunnelling and Underground Space Technology*, 18(2-3), pp. 233–241. 2003. [https://doi.org/10.1016/S0886-7798\(03\)00032-4](https://doi.org/10.1016/S0886-7798(03)00032-4)
- [18] Teachavorasinskun, S., Chub-Uppakarn, T. "Experimental verification of joint effects on segmental tunnel lining". *Electronic Journal of Geotechnical Engineering*, 14, pp. 1–8. 2008. <https://www.scribd.com/document/262427604/Experimental-Verification-of-Joint-Effects-on-Segmental-Tunnel-Lining#>
- [19] Teachavorasinskun, S., Chub-uppakarn, T. "Influence of segmental joints on tunnel lining". *Tunnelling and Underground Space Technology*, 25(4), pp. 490–494. 2010. <https://doi.org/10.1016/j.tust.2010.02.003>
- [20] Molins, C., Arnau, O. "Experimental and analytical study of the structural response of segmental tunnel linings based on an in situ loading test.: Part 1: Test configuration and execution". *Tunnelling and Underground Space Technology*, 26(6), pp. 764–777. 2011. <https://doi.org/10.1016/j.tust.2011.05.002>
- [21] Bilotta, E., Russo, G. "Internal forces arising in the segmental lining of an earth pressure balance-bored tunnel". *Journal of Geotechnical and Geoenvironmental Engineering*, 139(10), pp. 1765–1780. 2013. [https://doi.org/10.1061/\(ASCE\)GT.1943-5606.0000906](https://doi.org/10.1061/(ASCE)GT.1943-5606.0000906)
- [22] Ye, F., Gou, C.-f., Sun, H.-d., Liu, Y.-p., Xia, Y.-x., Zhou, Z. "Model test study on effective ratio of segment transverse bending rigidity of shield tunnel". *Tunnelling and Underground Space Technology*, 41, pp. 193–205. 2014. <https://doi.org/10.1016/j.tust.2013.12.011>

- [23] Salemi, A., Esmaili, M., Sereshki, F. "Normal and shear resistance of longitudinal contact surfaces of segmental tunnel linings". *International Journal of Rock Mechanics and Mining Sciences*, 77, pp. 328–338. 2015. <https://doi.org/10.1016/j.ijrmmms.2015.04.014>
- [24] Augarde, C., Burd, H. "Three-dimensional finite element analysis of lined tunnels". *International Journal for Numerical and Analytical Methods in Geomechanics*, 25(3), pp. 243–262. 2001. <https://doi.org/10.1002/nag.127>
- [25] Hefny, A. M., Chua, H. C. "An investigation into the behaviour of jointed tunnel lining". *Tunnelling and Underground Space Technology*, 21(3–4), p. 428. 2006. <https://doi.org/10.1016/j.tust.2005.12.070>
- [26] Chen, J., Mo, H. "Numerical study on crack problems in segments of shield tunnel using finite element method". *Tunnelling and Underground Space Technology*, 24(1), pp. 91–102. 2009. <https://doi.org/10.1016/j.tust.2008.05.007>
- [27] Arnau, O., Molins, C. "Experimental and analytical study of the structural response of segmental tunnel linings based on an in situ loading test. Part 2: Numerical simulation". *Tunnelling and Underground Space Technology*, 26(6), pp. 778–788. 2011. <https://doi.org/10.1016/j.tust.2011.04.005>
- [28] Arnau, O., Molins, C. "Three dimensional structural response of segmental tunnel linings". *Engineering Structures*, 44, pp. 210–221. 2012. <https://doi.org/10.1016/j.engstruct.2012.06.001>
- [29] Do, N.-A., Dias, D., Oreste, P., Djeran-Maigre, I. "2D numerical investigation of segmental tunnel lining under seismic loading". *Soil Dynamics and Earthquake Engineering*, 72, pp. 66–76. 2015. <https://doi.org/10.1016/j.soildyn.2015.01.015>
- [30] Kim, C. Y., Bae, G., Hong, S., Park, C., Moon, H., Shin, H. "Neural network based prediction of ground surface settlements due to tunnelling". *Computers and Geotechnics*, 28(6-7), pp. 517–547. 2001. [https://doi.org/10.1016/S0266-352X\(01\)00011-8](https://doi.org/10.1016/S0266-352X(01)00011-8)
- [31] Leu, S.-S., Chen, C.-N., Chang, S.-L. "Data mining for tunnel support stability: neural network approach". *Automation in Construction*, 10(4), pp. 429–441. 2001. [https://doi.org/10.1016/S0926-5805\(00\)00078-9](https://doi.org/10.1016/S0926-5805(00)00078-9)
- [32] Benardos, A., Kaliampakos, D. "Modelling TBM performance with artificial neural networks". *Tunnelling and Underground Space Technology*, 19(6), pp. 597–605. 2004. <https://doi.org/10.1016/j.tust.2004.02.128>
- [33] Gajewski, J., Jonak, J. "Utilisation of neural networks to identify the status of the cutting tool point". *Tunnelling and Underground Space Technology*, 21(2), pp. 180–184. 2006. <https://doi.org/10.1016/j.tust.2005.07.003>
- [34] Majdi, A. "Prediction of triaxial compressive strength of intact rock samples by artificial neural network". Paper presented at the Geotechnical Conference, Ottawa, Canada, December, 2007.
- [35] Majdi, A., Beiki, M. "Evolving neural network using a genetic algorithm for predicting the deformation modulus of rock masses". *International Journal of Rock Mechanics and Mining Sciences*, 47(2), pp. 246–253. 2010. <https://doi.org/10.1016/j.ijrmmms.2009.09.011>
- [36] Majdi, A., Rezaei, M. "Application of Artificial Neural Networks for Predicting the Height of Destressed Zone Above the Mined Panel in Longwall Coal Mining". In: 47th US Rock Mechanics/Geomechanics Symposium of Conference. American Rock Mechanics Association. 2013.
- [37] Majdi, A., Rezaei, M. "Prediction of unconfined compressive strength of rock surrounding a roadway using artificial neural network". *Neural Computing and Applications*, 23(2), pp. 381–389. 2013. <https://doi.org/10.1007/s00521-012-0925-2>
- [38] Beiki, M., Majdi, A., Givshad, A. D. "Application of genetic programming to predict the uniaxial compressive strength and elastic modulus of carbonate rocks". *International Journal of Rock Mechanics and Mining Sciences*, 63, pp. 159–169. 2013. <https://doi.org/10.1016/j.ijrmmms.2013.08.004>
- [39] Rezaei, M., Majdi, A., Monjezi, M. "An intelligent approach to predict unconfined compressive strength of rock surrounding access tunnels in longwall coal mining". *Neural Computing and Applications*, 24(1), pp. 233–241. 2014. <https://doi.org/10.1007/s00521-012-1221-x>
- [40] Santos, O. J., Celestino, T. B. "Artificial neural networks analysis of Sao Paulo subway tunnel settlement data". *Tunnelling and Underground Space Technology*, 23(5), pp. 481–491. 2008. <https://doi.org/10.1016/j.tust.2007.07.002>
- [41] Tiriyaki, B. "Application of artificial neural networks for predicting the cuttability of rocks by drag tools". *Tunnelling and Underground Space Technology*, 23(3), pp. 273–280. 2008. <https://doi.org/10.1016/j.tust.2007.04.008>
- [42] Shi, B. H., Li, W. Q. "Online Fault Prediction for EPB Shield Tunneling Based on Neural Network". *Advanced Materials Research*, 457–458, pp. 1287–1293. 2012. <https://doi.org/10.4028/www.scientific.net/AMR.457-458.1287>
- [43] Ford, H., Alexander, J. M. "Advanced mechanics of materials", 672 p. Longmans, London. 1963. <https://www.amazon.com/Advanced-mechanics-materials-Hugh-Ford/dp/B0007EAU3G>
- [44] Wikipedia. "Von Mises yield criterion.". 2016. https://en.wikipedia.org/w/index.php?title=Von_Mises_yield_criterion&oldid=719261117
- [45] Fausett, L. "Fundamentals of neural networks: architectures, algorithms, and applications". Prentice-Hall, Inc. 1994. <https://www.amazon.com/Fundamentals-Neural-Networks-Architectures-Applications/dp/0133341860>
- [46] Rosenblatt, F. "The perceptron: a probabilistic model for information storage and organization in the brain". *Psychological Review*, 65(6), 386–408. 1958. <https://doi.org/10.1037/h0042519>
- [47] Rumelhart, D. E., Hinton, G. E., Williams, R. J. "Learning representations by back-propagating errors". *Cognitive modeling*, 5(3):1. 1988.
- [48] Lawrence, J. "Introduction to neural networks". California Scientific Software, Nevada City, CA, USA. 1993. <http://dl.acm.org/citation.cfm?id=184210>
- [49] Flood, I., Kartam, N. "Neural networks in civil engineering. I: Principles and understanding.". *Journal of Computing in Civil Engineering*, 8(2), pp. 131–148. 1994. [https://doi.org/10.1061/\(ASCE\)0887-3801\(1994\)8:2\(131\)](https://doi.org/10.1061/(ASCE)0887-3801(1994)8:2(131))
- [50] Cybenko, G. "Approximation by superpositions of a sigmoidal function". *Mathematics of Control, Signals and Systems*, 2(4), pp. 303–314. 1989. <https://doi.org/10.1007/BF02551274>
- [51] Pawtucket, P., R.I., ABAQUS. Abaqus Inc., . 2014
- [52] Department of the Army, U.S. Army Corps of Engineers. "Tunnels and Shafts in Rock EM 1110-2-2901.". Engineer Manual, Washington, DC. 1997. https://www.ita-aites.org/media/k2/attachments/public/3_Tunnels%20and%20Shafts%20in%20Rock%20by%20US%20Army%20CE.pdf
- [53] Rojas, R. "Neural networks: a systematic introduction". 502 p. Springer Science & Business Media, Berlin, Heidelberg. 2013. <https://books.google.hu/books?id=4rESBwAAQBAJ&printsec=frontcover#v=onepage&q&f=false>
- [54] Etzkorn, B. (2011) Data Normalization and Standardization.
- [55] Hush, D. R. "Classification with neural networks: a performance analysis.". In: Systems Engineering 1989, IEEE International Conference on. IEEE, 24–26 August 1989. <https://doi.org/10.1109/ICSYSE.1989.48672>
- [56] Hecht-Nielsen, R. "Kolmogorov's mapping neural network existence theorem". In: Proceedings of the International Conference on Neural Networks. pp. 11–13. IEEE Press, New York. 1987.
- [57] Kanellopoulos, I., Wilkinson, G. "Strategies and best practice for neural network image classification". *International Journal of Remote Sensing*, 18(4), pp. 711–725. [10.1080/014311697218719](https://doi.org/10.1080/014311697218719)
- [58] Wang, C. "A theory of generalization in learning machines with neural network applications". Doctoral dissertation, University of Pennsylvania Philadelphia, PA, USA. 1994. <http://dl.acm.org/citation.cfm?id=921726>

- [59] Masters, T., Schwartz, M. "Practical neural network recipes in C". *IEEE Transactions on Neural Networks*, 5(5):853–853. 1994.
- [60] Grima, M. A. "Neuro-fuzzy modeling in engineering geology". 244 p. AA Balkema, Rotterdam. 2000.
- [61] Ross, T. J. "Fuzzy logic with engineering applications". John Wiley & Sons. 2009.
- [62] Habibagahi, G., Katebi, S. "Rock mass classification using fuzzy sets". *Iranian Journal of Science and Technology Transactions B-Engineering*, 20(3), pp. 273–284. 1996. <http://en.journals.sid.ir/ViewPaper.aspx?ID=24069>
- [63] Den Hartog, M., Babuška, R., Deketh, H., Grima, M. A., Verhoef, P., Verbruggen, H. B. "Knowledge-based fuzzy model for performance prediction of a rock-cutting trencher.". *International Journal of Approximate Reasoning*, 16(1), pp. 43–66. 1997. [https://doi.org/10.1016/S0888-613X\(96\)00118-1](https://doi.org/10.1016/S0888-613X(96)00118-1)